IGF-1R inhibition enhances radiosensitivity and delays double-strand break repair by both non-homologous end-joining and homologous recombination.

Chitnis et al

Supplemental methods

Cell culture

DU145, 22Rv1 and LNCaP-LN3 cells were cultured in RPMI-1640 medium and PC3 cells in Ham's F12 medium. LNCaP-LN3 cells were used in preference to parental LNCaP cells because the LNCaP-LN3 subline is more firmly adherent, so less subject to detachment during chemical treatment or irradiation. R− and R+ cells were cultured in Dulbecco's Modified Eagle medium (DMEM), and M059J and M059K cells in 1:1 Ham's F12:DMEM with 1% pyruvate, 1% non-essential amino acids (Gibco/Life Technologies Ltd., UK). All media were supplemented with 10% fetal calf serum (FCS) and 100 units/ml of penicillin and streptomycin. R− and R+ cell medium also contained 50μg/ml geneticin sulphate (Gibco/Life Technologies Ltd., UK). HEK-293 EJ5-GFP/TST and HEK293 DR-GFP/TST cells were cultured in phenol red free DMEM with 10% charcoal-stripped FCS, 100 units/ml of penicillin/streptomycin, 1μg/ml puromycin and 5μg/ml blasticidin. All cell lines tested negative for mycoplasma infection using the MycoAlert detection kit (Lonza, UK).

Western blotting

The following primary antibodies were used for western blotting: IGF-1Rβ (#3027, Cell Signaling Technology, CST), phospho-Y1135/6 IGF-1R (#3024, CST), insulin receptor (#3025, CST), IRS-1 (#2382, CST), phospho-S473 AKT (#4051, CST), AKT (#9272, CST), phospho-T202/Y204 ERK 1/2 (#4377, CST), ERK 1/2 (#4695, CST), PTEN (#9556, CST), androgen receptor (#3202, CST), S139 γH2AX (#2577, CST), phospho-S1981 ATM (#4526, CST), ATM (#2872, CST), phospho-S2056 DNA-PKcs (#ab18192, Abcam), DNA-PKcs (#4602, CST), Ku70 and 80 (MS-329-P0 and MS-285-P0, Thermo-Scientific), ligase

IV (AbD Serotec), XRCC4 (#ab2857, Abcam), XLF (#2854, CST), MRE11 (#4895, CST), RAD50 (MAI-23269, Thermo-Scientific), RAD51 (#ab213, Abcam), NBS1 (#3002, CST), BRCA1 (#ab16780, Abcam), RPA32 (#ab10359, Abcam), phospho-S824 KAP-1 (#A300-274A, Bethyl Lab. Inc), KAP-1 (#A300-767A, Bethyl Lab. Inc), phospho-T68 Chk-2 (#2661, CST), Chk-2 (#2662, CST), phospho-S15 p53 (#9284, CST), β-tubulin (#T4026, Sigma) and myosin IIb (#3404, CST).

Supplementary Tables

Supplementary Table S1

	Control			AZ12253801		
Time (hr)	G1 (%)	S (%)	G2/M (%)	G1 (%)	S (%)	G2/M (%)
1	54.1 ± 5.1	31.0 ± 4.1	12.5 ± 4.0	53.2 ± 6.7	31.0 ± 5.0	14.3 ± 3.8
4	44.1 ± 5.6	31.7 ± 4.0	14.5 ± 8.0	46.6 ± 4.5	33.7 ± 7.8	16.8 ± 7.0
8	55.2 ± 11.6	18.3 ± 1.0	25.1 ± 11.7	47.2 ± 7.7	19.8 ± 1.6	26.9 ± 12.6
18	59.3 ± 4.2	21.8 ± 2.3	22.5 ± 3.1	59.8 ± 2.2	20.7 ± 2.7	18.7 ± 5.0
24	52.1 ± 8.0	21.7 ± 1.7	13.0 ± 6.1	55.6 ± 7.3	21.0 ± 3.7	14.7 ± 7.2
48	42.3 ± 13.1	24.2 ± 11.3	26.1 ± 5.0	43.3 ± 13.7	22.5 ± 11.3	25.9 ± 5.6

	Control + IR			AZ12253801 + IR		
Time (hr)	G1 (%)	S (%)	G2/M (%)	G1 (%)	S (%)	G2/M (%)
0	48.8 ± 1.2	32.7 ± 5.3	17.7 ± 3.9	48.0 ± 2.4	33.6 ± 1.3	14.4 ± 1.5
1	47.1 ± 3.8	36.9 ± 2.1	13.5 ± 2.2	46.2 ± 3.2	36.9 ± 2.6	15.8 ± 2.3
4	39.5 ± 4.0	37.9 ± 2.8	21.7 ± 1.8	37.4 ± 3.1	36.3 ± 2.3	23.5 ± 1.9
6	30.9 ± 4.2	35.4 ± 1.9	31.1 ± 7.0	32.1 ± 2.7	32.9 ± 2.5	31.7 ± 3.9
8	30.3 ± 4.4	34.2 ± 1.3	34.2 ± 6.6	27.5 ± 5.2	33.8 ± 0.6	35.4 ± 8.2
18	54.1 ± 5.0	27.2 ± 7.0	15.8 ± 1.2	54.5 ± 0.9	15.8 ± 4.6	25.2 ± 6.4
24	61.4 ± 5.6	22.5 ± 4.7	14.9 ± 2.3	63.2 ± 2.3	20.8 ± 2.8	13.5 ± 1.2

Legend to Supplementary Table 1: AZ12253801 does not influence cell cycle distribution within 48hr of irradiation. Upper: DU145 cells were treated with solvent or 30nM AZ12253801 for 4 hours. At 1-48hr after the 4hr incubation, cells were fixed and PI stained for cell cycle analysis, and FlowJo 7.6.5 software was used to assign G1, S and G2/M phases. Table shows % cells in each cell cycle phase, expressed as mean ± SEM of triplicate values from 3 independent experiments. There were no significant differences by t-test between mean values for control and 30nM AZ12253801-treated cells. **Lower:** cells were treated with solvent or 30nM AZ12253801 for 4hr, irradiated (3Gy) and harvested at intervals for cell cycle analysis. No significant differences were found between control and AZ12253801-treated cells.

Supplementary Table S2

AZ12253801 nM	**G1 (%)**	**S (%)**	**G2/M (%)**
0	57.6 ± 0.5	16.8 ± 0.5	25.6 ± 0.5
30	47.4 ± 0.6	20.6 ± 1.3	31.9 ± 0.9
60	45.0 ± 0.7	20.2 ± 0.4	34.8 ± 0.3

Legend to Supplementary Table S2. Effects of AZ12253801 on cell cycle distribution of NHEJ reporter HEK293 cells. Triplicate samples of solvent (control) or AZ12253801-treated EJ5-GFP-TST HEK293 cells were subject to cell cycle analysis as Supplementary Figure S6. Table: mean ± SEM % cells in each cell cycle phase.

Legends to Supplementary Figures

Figure S1 AZ12253801 SF_{50} interpolation in R+ cells. R+ cell survival data from Figure 1c plotted with linear y-axis to show SF_{50} interpolation.

Figure S2 Effect of IGF-1R inhibition on radiosensitivity of PC3, 22Rv1 and LNCaP-LN3 cells. Cells were treated with solvent, AZ12253801 at or below the SF_{50} for each cell line, or 3μM ATM inhibitor KU55933. After 11-12 days, visible colonies were stained and counted, and cell survival was expressed as % survival in solvent-treated controls. Points represent the mean ± SEM for triplicate values from three independent experiments in each cell line. In PC3 cells, AZ12253801 at 30nM enhanced sensitivity to 3 Gy (*$p<0.05$) and at 60nM to 1 Gy ($p<0.05$), 3 Gy ($p<0.01$) and 5 Gy ($p<0.05$ by one way ANOVA). KU55933 also radiosensitized PC3 cells ($p<0.001$ at 3 Gy, $p<0.05$ at 5 Gy compared with control-treated cells) but did not show statistically significant radiosensitization compared with 30 or 60 nM AZ12253801. In 22Rv1 cells, 30nM AZ12253801 enhanced sensitivity to 1 and 3 Gy ($p<0.01$), effects that were not significantly different from radiosensitization induced by ATM inhibition. AZ12253801-pre-treated LNCaP-LN3 cells showed minor enhancement of sensitivity to 1 Gy (52 ± 3% survival compared with 64 ± 2% in controls, $p<0.05$), but there were no differences at 3-5 Gy and no change in radiosensitivity in cells treated with KU55933.

Figure S3 Radiosensitization of DU145 cells by IGF-1R inhibition is unaccompanied by early (≤48hr) changes in cell cycle profile or apoptosis, or by senescence. a) Representative cell cycle profiles from DU145 cells treated with: upper, solvent (control) or 30nM AZ12253801 for 4hr then collected at intervals of 1-24hr; lower: treated for 4hr with solvent or AZ12253801 as above, irradiated (3 Gy), and collected at intervals post-irradiation. FlowJo 7.6.5 software was used to assign G1, S and G2/M phases, and the data are summarized in Supplementary Table S1.

b) DU145 cells were treated with solvent or left: 30nM; right: 60nM AZ12253801 for 4 hr prior to 3Gy irradiation. At time-points up to 48hrs post-irradiation, cells were analysed for apoptosis using the Apo-1 Homogeneous Caspase-3/7 apoptosis assay. Graphs show fluorescence units expressed as % increase above solvent treated controls. Points represent mean increase ± SEM in triplicate wells in two independent experiments. There were significant increases in apoptosis induction in irradiated controls vs AZ12253801-treated cells (**$p<0.01$, ***$p<0.001$ by one-way ANOVA), but no significant differences in apoptosis between irradiated and irradiated/IGF-1R inhibited cells. **c)** DU145 cells were treated with solvent or AZ12253801, after 4hr irradiated (3Gy), and after a further 24hr assayed for senescence-associated β-galactosidase in parallel with visibly senescent primary renal cell cancer (RCC) cells as positive controls. Experiments were repeated 3 times and representative cells are shown, original magnification x10. Primary RCC cells showed β-galactosidase staining, but there was no staining and no change in cell morphology in AZ12253801-treated DU145 cells. Similar analyses were performed 1-11 days following 1-10 Gy irradiation (not shown), with no evidence of β-galactosidase activity in DU145 cells.

Figure S4: Detection of irradiation-induced γH2AX foci in DU145 and LNCaP-LN3 cells. a) DU145 cells were mock irradiated or irradiated, and 1hr later fixed and stained for γH2AX. Foci were counted in ≥30 cells for each condition and expressed as mean ± SEM foci per cell. **b)** DU145 cells were irradiated at 3Gy and 1hr post irradiation cells were fixed and stained for γH2AX (green), 53BPI (red), and DAPI (blue). Original magnification x40. **c)** LNCaP-LN3 cells were treated with solvent (Control) or AZ12253801 at 20nM, the SF_{50} for this cell line (Table 1). After 4hr, cells were irradiated (3Gy), and at intervals fixed and stained for S139 γH2AX to quantify γH2AX foci as Legend to Figure 4c, d. Graph shows mean ± SEM foci in ≥60 cells per condition.

Figure S5: Investigating basis for radiosensitization induced by IGF-1R inhibition. **a)** Serum-starved DU145 cells were treated with 50nM IGF-1 for 15min and then lyzed, or irradiated (5Gy) and lyzed 1hr post irradiation with solvent or IGF-1 treatment in the final 15min. Precleared lysates were immunoprecipitated with: left, IGF-1R antibody; right, IRS-1 antibody, or irrelevant control antibody (C). IPs were analyzed by western blotting for DNAPKcs and ATM. **b)** DU145 cells were treated for 4 hours with solvent, 30nM IGF-1R inhibitor AZ12253801 (AZ3801) or 10μM ATM inhibitor KU55933, irradiated (5Gy), lysed in SDS lysis buffer one hour post irradiation, and analysed for markers of ATM activation: ATM S1981 autophosphorylation, and phosphorylation of KAP-1, Chk2, p53 and γH2AX. The ATM dependence of these phosphorylations was confirmed by the response to KU55933. Dashed line indicates removal of 3 intervening lanes. The results are representative of three independent analyses. **c)** M059J and K cells were treated with 3μM KU55933 (ATM inhibitor) for 4hr, irradiated, and after 11-12 days, visible colonies were stained and counted. Cell survival was expressed as % survival in unirradiated controls. Points represent the mean ± SEM for triplicate values in three separate experiments. ATM inhibition enhanced radiosensitivity of M059K cells at 1 ($p<0.01$), 3 ($p<0.001$) and 5 Gy ($p<0.001$), and M059J cells at 1 ($p<0.05$), 3 ($p<0.001$) and 5 Gy ($p<0.001$). **d)** DU145 cells were treated with ATM inhibitor KU55933 or DNA-PK inhibitor NU7441 for 4hrs, irradiated, and 1hr later lysed for western blot to assess phosphorylation of ATM effectors Chk2 and KAP-1.

Figure S6: Effect of AZ12253801 on cell cycle profiles of HEK293 repair reporter cells. EJ5-GFP-TST HEK293 cells were treated with solvent or AZ12253801 as Figure 6, in parallel with cultures used for repair assays. After 72hr, cell cycle profiles were determined as in Figure S3, and the data are summarized in Supplementary Table S2.

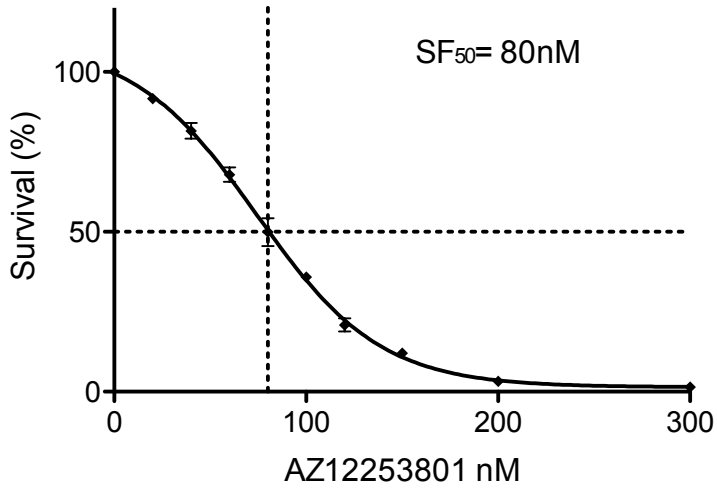
SF50= 80nM
100
50
0
Survival (%)
0
100
200
300
AZ12253801 nM

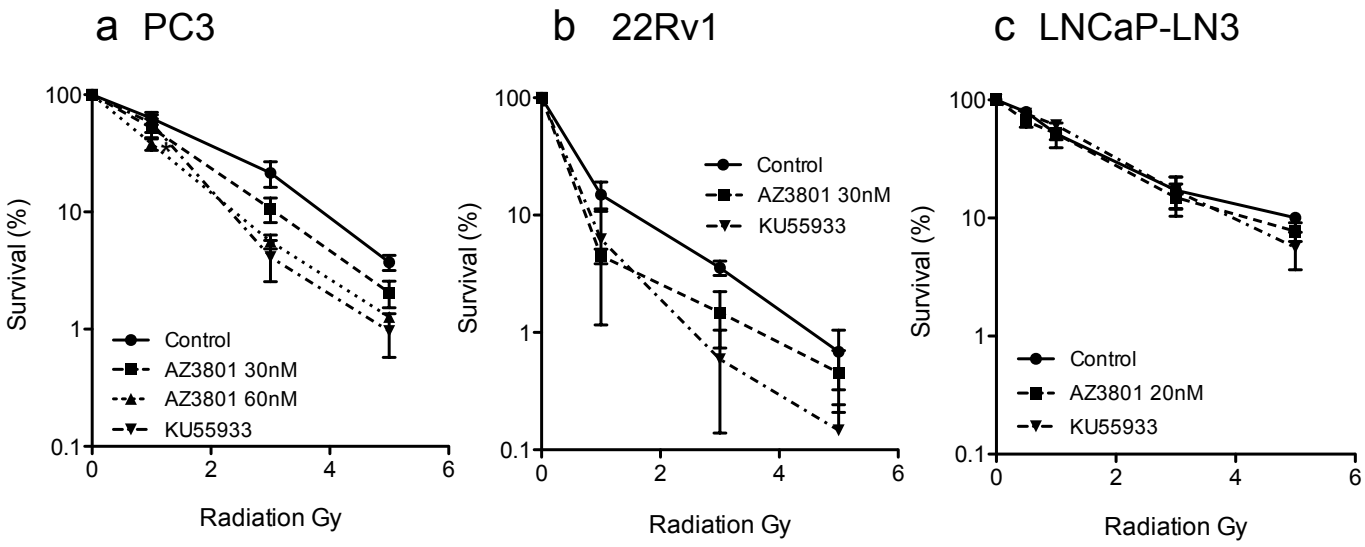
a PC3
b 22Rv1
c LNCaP-LN3
Survival (%)
Radiation Gy
Control
AZ3801 30nM
AZ3801 60nM
KU55933
AZ3801 20nM
100
10
1
0.1
0
2
4
6

a

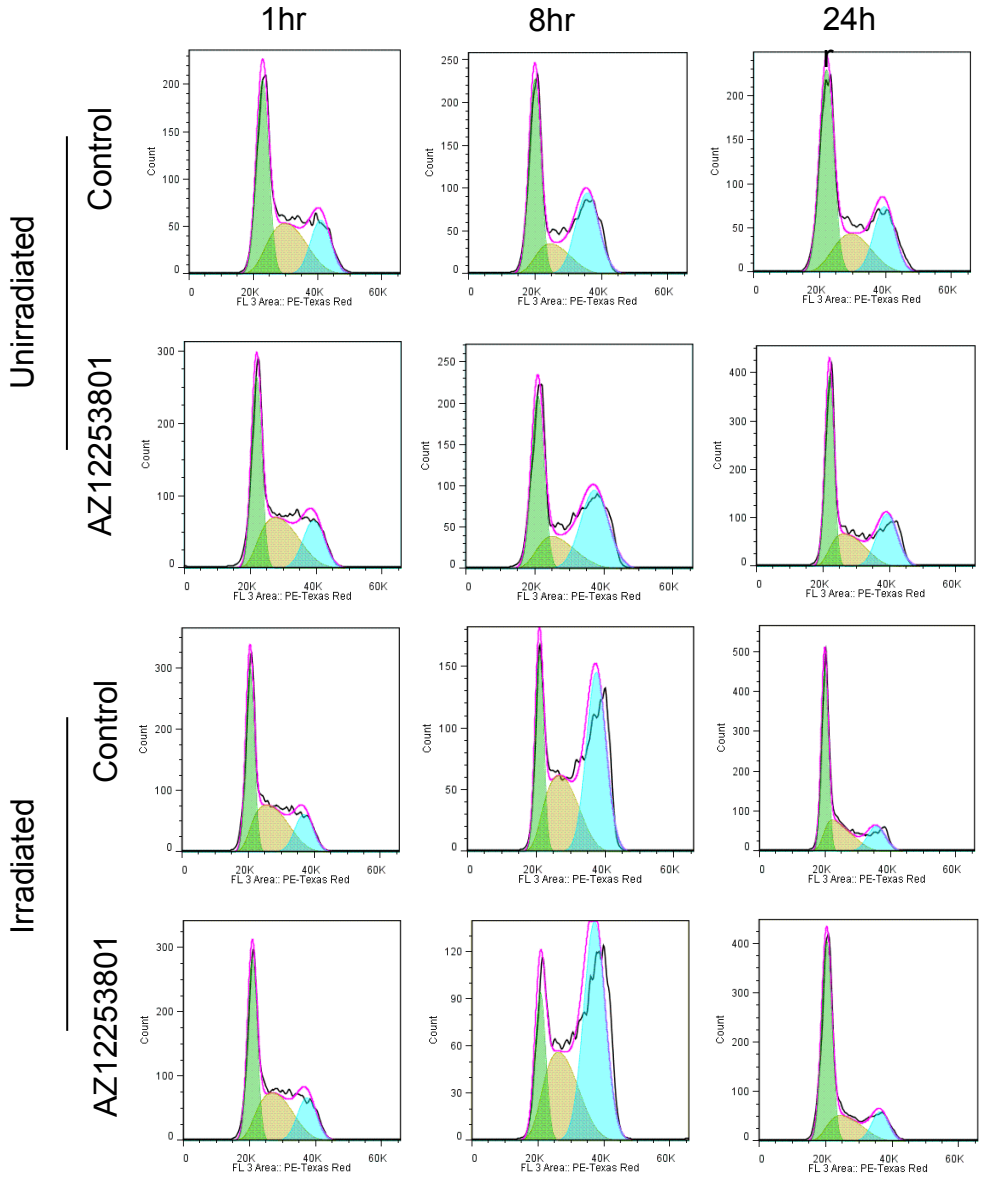
1hr
8hr
24h
Unirradiated
Control
AZ12253801
Irradiated
Control
AZ12253801
Count
FL 3 Area:: PE-Texas Red

b

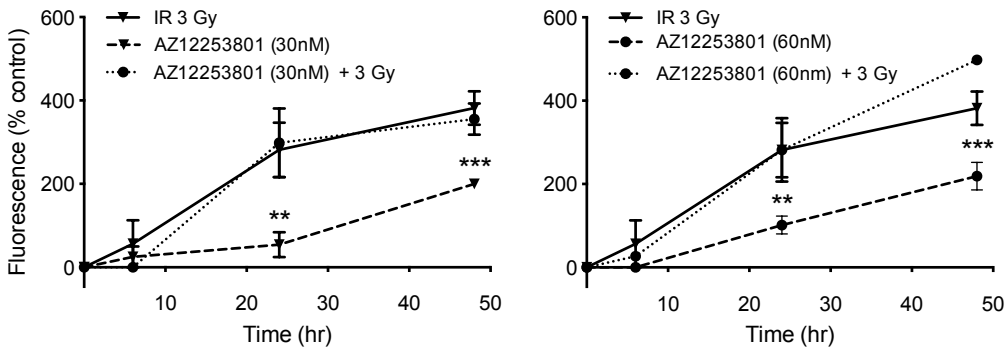
IR 3 Gy
AZ12253801 (30nM)
AZ12253801 (30nM) + 3 Gy
AZ12253801 (60nM)
AZ12253801 (60nm) + 3 Gy
Fluorescence (% control)
Time (hr)
**
***

c

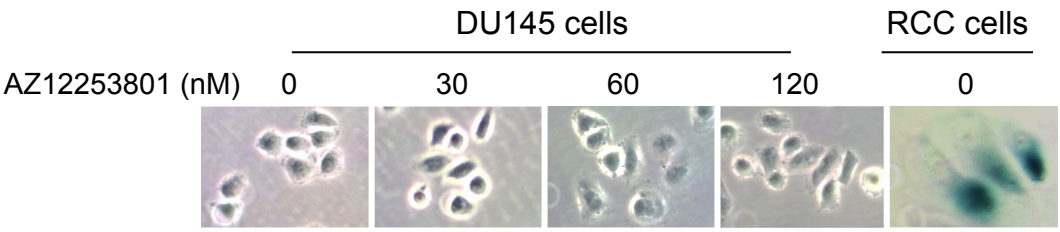
DU145 cells
RCC cells
AZ12253801 (nM)
0
30
60
120
0

a

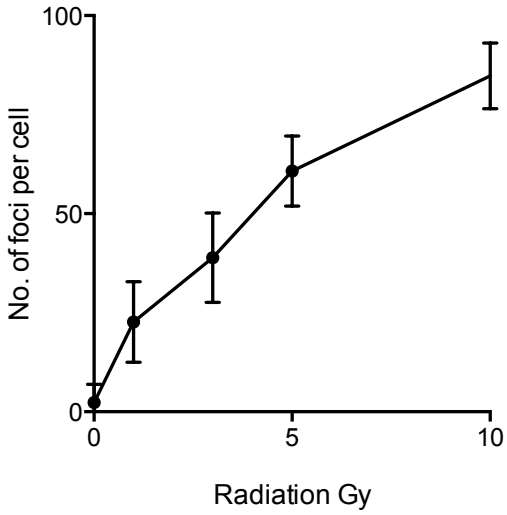
100
50
0
No. of foci per cell
0
5
10
Radiation Gy

b

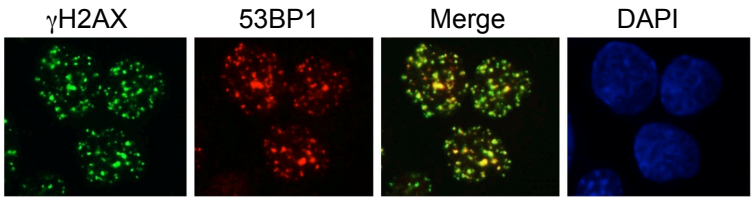
γH2AX
53BP1
Merge
DAPI

c

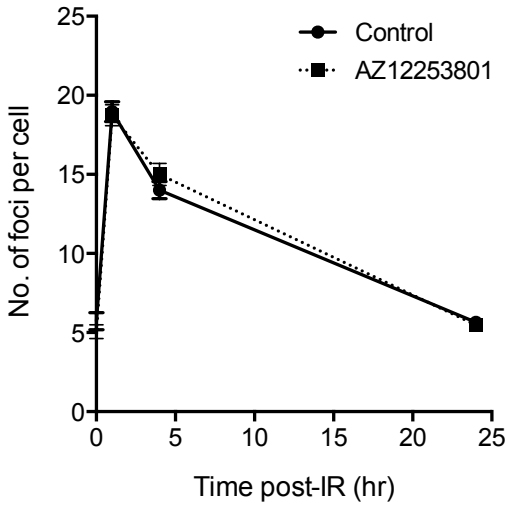
25
20
15
10
5
0
No. of foci per cell
Control
AZ12253801
0
5
10
15
20
25
Time post-IR (hr)

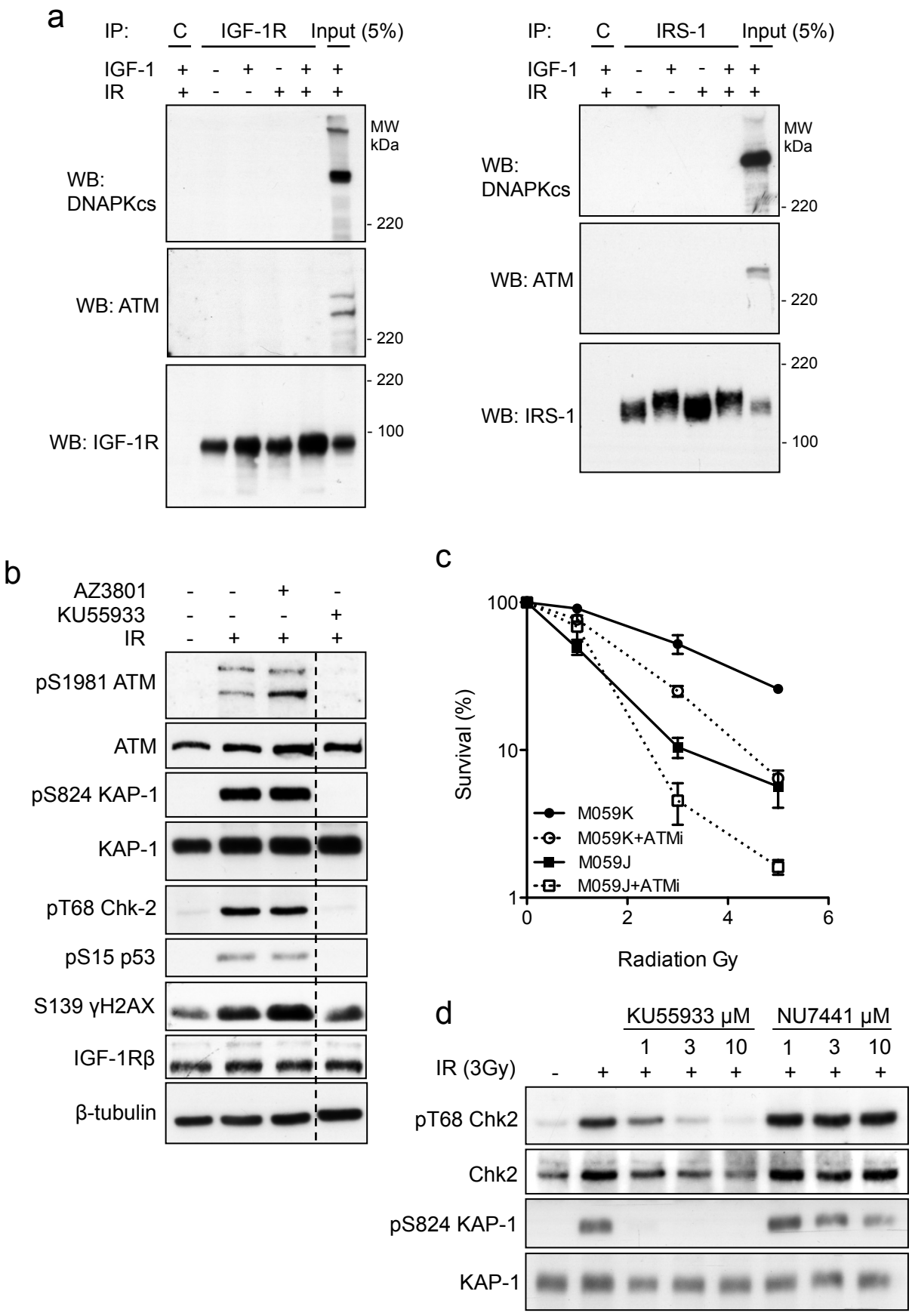
a
IP: C IGF-1R Input (5%)
IGF-1 + - + - + +
IR + - - + + +
MW kDa
WB: DNAPKcs
220
WB: ATM
220
220
WB: IGF-1R
100
IP: C IRS-1 Input (5%)
IGF-1 + - + - + +
IR + - - + + +
MW kDa
WB: DNAPKcs
220
WB: ATM
220
220
WB: IRS-1
100
b
AZ3801 - - + -
KU55933 - - - +
IR - + + +
pS1981 ATM
ATM
pS824 KAP-1
KAP-1
pT68 Chk-2
pS15 p53
S139 γH2AX
IGF-1Rβ
β-tubulin
c
100
10
1
Survival (%)
0
2
4
6
Radiation Gy
M059K
M059K+ATMi
M059J
M059J+ATMi
d
KU55933 μM
NU7441 μM
1 3 10 1 3 10
IR (3Gy) - + + + + + + +
pT68 Chk2
Chk2
pS824 KAP-1
KAP-1

Supplementary Figure S6

Chitnis et al